PHYSICAL REVIEW C VOLUME 7, NUMBER 3 MARCH 1973

Shell-Model Calculations for $A = 18$, 19, and 20 Nuclei with Core Excitation Included Explicitly

J. B. McGrory
Oak Ridge National Laboratory, Oak Ridge, Tennessee 37830*

and

B. H. Wildenthal†
Cyclotron Laboratory, Department of Physics, Michigan State University, East Lansing, Michigan 48823
(Received 25 October 1972)

Eigenvalues and eigenvectors for all low-lying positive- and negative-parity nuclear states of $A=18$, 19, and 20 are calculated in a shell-model basis of all Pauli-allowed $0p_{1/2}$-$0d_{5/2}$-$1s_{1/2}$ configurations outside an inert ^{12}C core. Two different effective Hamiltonians are used. One is based on a reaction matrix treatment of the Hamada-Johnston potential. The second one is obtained by varying the 33 effective Hamiltonian matrix elements to reach a least-squares fit between 153 experimental level energies in nuclei in the $A=13$–22 region and the corresponding shell-model eigenvalues. The energy level spectra and single-nucleon spectroscopic factors from these calculations are compared to the available experimental data in this region. The calculations are also examined for the existence and characteristics of sequences of levels which might be called "rotational bands."

I. INTRODUCTION

The conventional nuclear shell model has been applied with considerable success to the study of properties of low-lying states of nuclei at the beginning ($A=18$–22) of what is called the s-d shell.[1] In these calculations, an inert ^{16}O is assumed, and active particles are distributed in the $0d_{5/2}$, $1s_{1/2}$, and $0d_{3/2}$ single-particle orbits. This model is obviously limited, since there is ample evidence that ^{16}O is not an ideal closed-shell nucleus. Some of this evidence involves the existence of excited states in the observed spectrum of ^{16}O and the existence of negative-parity states at low excitation energies in $A=17$, 18, and 19 nuclei. Zuker, Buck, and McGrory[2] (ZBM) have studied the structure of ^{16}O in a conventional shell-model calculation with the assumption of an inert ^{12}C core and active $0d_{5/2}$, $1s_{1/2}$, and $0p_{1/2}$ orbits. In this model space, there exist numerous excited states in the $A=16$ system, and the ZBM calculation accounted for many of the observed properties of the spectrum of ^{16}O below 15 MeV. Calculations in this same model space were subsequently made for ^{17}O and for the $A=18$ system,[3,4] in each case with considerable success.

There are many interesting properties of nuclei with $A=19$ and 20 which cannot be explained by the conventional shell model with an inert ^{16}O core. These include the existence of an apparent $K=\frac{1}{2}^-$ rotational band of states in ^{19}F which is all but degenerate with the ground-state $K=\frac{1}{2}^+$ band in that nucleus, the observed "extra" 0^+ and 2^+ states in ^{20}Ne between 6 and 8 MeV, the existence of possibly two low-lying negative-parity rotational bands in ^{20}Ne, and the occurrence of several states in observed spectrum of ^{20}F which do not occur in any "good" shell-model calculation with an ^{16}O core. It is of interest to see if the ^{16}O-core-excited model which accounts so well for the properties of ^{16}O, ^{17}O, and the $A=18$ nuclei can account for some of these "anomalous" properties of $A=19$ and 20 nuclei. A preliminary study has indicated that such is the case.[5] In the present paper, we present in some detail the results of calculations for nuclei with $A=18$–20 in terms of a $0p_{1/2}$-$0d_{5/2}$-$1s_{1/2}$ ("pds") configuration shell model. We restrict ourselves here to discussion of excitation energies and spectroscopic factors for single-nucleon transfer reactions, deferring to a later paper a discussion of electromagnetic properties of states in these nuclei as calculated in terms of this model.

In Sec. II, we describe the calculation in detail. In Sec. III we present a nucleus-by-nucleus discussion of energy levels and spectroscopic factors. In Sec. IV we briefly discuss the core excitation present in the model calculations. In Sec. V, we compare our calculations with other calculations of these nuclei. The results are summarized in Sec. VI.

II. DESCRIPTION OF THE CALCULATIONS

In the following sections, we will discuss the results of three different shell-model calculations of the properties of low-lying states in $A=18$–20 nuclei. In two of the calculations an inert ^{12}C is

assumed, and the $0d_{5/2}$, $1s_{1/2}$, and $0p_{1/2}$ orbits comprise the active model space. For a nucleus with A nucleons, we include all Pauli-allowed states of $A-12$ particles distributed in these three active orbits. Thus, for ^{20}Ne, we distribute eight particles in the $d_{5/2}$, $s_{1/2}$, and $p_{1/2}$ orbits. We include configurations with any possible number of particles excited from the $p_{1/2}$ orbit to the $d_{5/2}$ and $s_{1/2}$ orbits. Thus, for positive-parity states, we include all configurations with 0, 2, and 4 holes in the $p_{1/2}$ shell, and for negative-parity states we include all configurations with 1 and 3 holes in the $p_{1/2}$ orbit. Within the space of these states we diagonalize an effective one-body plus two-body Hamiltonian. The resulting eigenvalues are correlated with energy levels, and the resulting eigenvectors are used in the calculation of spectroscopic factors for single-nucleon transfer reactions. These calculations are completely analogous to the shell-model calculations for $A = 16$, 17, and 18 previously mentioned.[2-5]

The two *pds*-model calculations differ in the effective Hamiltonians which are employed. For one set of calculations we use the interaction derived by Zuker[4] for $A = 18$. This interaction is constructed from realistic interactions determined for this mass region from free nucleon-nucleon potentials. The two-body matrix elements of the Hamiltonian were determined with minimal recourse to experimental level energies in the nuclei of interest. We will refer to the results obtained with this interaction with the adjective *Z-pds*.

The other set of *pds* calculations has been carried out with an effective interaction determined entirely by the observed level energies of the nuclei in this region. The two-body part of the effective Hamiltonian for the *pds*-model space is specified by 30 two-body matrix elements. The one-body part of the Hamiltonian is specified by three single-particle energies, which in this model are interpreted as the binding energies of particles in the three active orbits to the assumed inert ^{12}C core. We treated these 33 matrix elements as free parameters in a least-squares fit of shell-model eigenvalues to 19 ground state binding energies and 134 excitation energies of selected levels in nuclei with $A = 13-22$. The details of the data set and fit procedure are described elsewhere.[6] We will refer to the results calculated with this interaction with the adjective *F-pds*.

These two approaches to the determination of a shell-model effective interaction each have their advantages and disadvantages. The procedure for calculating so-called "realistic" interactions uses a perturbative approach which has been justified so far mostly on pragmatic grounds, i.e., more rigorous techniques are unavailable, and the results obtained are relatively successful vis-a-vis experiment. The use of the realistic interaction is more predictive in principle, since unlike the empirical search technique, the Hamiltonian is

TABLE I. The two-body matrix elements $\langle([lj]_1[lj]_2)_{JT}|V|([lj]_3[lj]_4)_{JT}\rangle$ for the *Z-pds*, *F-pds*, and *K-dsd* model Hamiltonians. The different orbits are identified by their orbital angular momenta l_i. Single particle energies:

Z-pds	3.50	2.75	0.0
F-pds	$0d_{5/2} = -1.67$,	$1s_{1/2} = -2.84$,	$0p_{1/2} = -5.70$
K-dsd	−4.15	−3.28	...

l_1	l_2	l_3	l_4	JT	Matrix element (MeV) *Z-pds*	*F-pds*	*K-dsd*	l_1	l_2	l_3	l_4	JT	Matrix element (MeV) *Z-pds*	*F-pds*	*K-dsd*
d	*d*	*d*	*d*	01	−2.41	−1.69	−2.44	*d*	*s*	*d*	*s*	31	1.16	1.64	0.17
d	*d*	*d*	*d*	10	0.01	−1.89	−1.03	*d*	*p*	*d*	*p*	20	−3.93	−4.15	
d	*d*	*d*	*d*	21	−1.21	−0.82	−1.04	*d*	*p*	*d*	*p*	21	0.71	0.78	
d	*d*	*d*	*d*	30	0.38	−2.08	−0.86	*d*	*p*	*d*	*p*	30	−2.58	−3.22	
d	*d*	*d*	*d*	41	−0.08	−0.32	−0.05	*d*	*p*	*d*	*p*	31	−0.34	−0.08	
d	*d*	*d*	*d*	50	−4.26	−4.33	−3.66	*s*	*s*	*s*	*s*	01	−1.67	−1.86	−1.95
d	*d*	*d*	*s*	21	−0.88	−1.23	−0.85	*s*	*s*	*s*	*s*	10	−3.17	−4.06	−3.18
d	*d*	*d*	*s*	30	−3.53	−2.89	−1.57	*s*	*s*	*p*	*p*	01	0.82	0.59	
d	*d*	*s*	*s*	01	−1.04	−1.03	−0.97	*s*	*s*	*p*	*p*	10	0.83	1.23	
d	*d*	*s*	*s*	10	−4.27	−3.26	−0.60	*s*	*p*	*s*	*p*	00	−3.48	−3.25	
d	*d*	*p*	*p*	01	3.37	3.76		*s*	*p*	*s*	*p*	01	1.67	2.19	
d	*d*	*p*	*p*	10	−1.20	−1.92		*s*	*p*	*s*	*p*	10	−1.28	−2.11	
d	*s*	*d*	*s*	20	−1.70	−2.19	−0.62	*s*	*p*	*s*	*p*	11	−0.24	0.41	
d	*s*	*d*	*s*	21	−1.17	−1.84	−1.29	*p*	*p*	*p*	*p*	01	−0.26	−0.29	
d	*s*	*d*	*s*	30	−2.60	−3.54	−3.69	*p*	*p*	*p*	*p*	10	−4.15	−4.47	

not directly determined by part of the data of interest.

The approach of determining the shell-model Hamiltonian directly from the level energy data is not encumbered with such problems as what diagrams to include in the renormalization procedure. In principle, it includes the correct renormalizations implicitly. It is obviously closely tied to the experimental data. On the other hand, it is difficult to determine precisely which parameters are unambiguously determined by the selected experimental data. This problem is closely tied to the problem of which levels should be included in the search, and how many levels comprise an adequate set. Again, after pointing to these problems, we appeal to the final results for justification of the procedures.

The third calculation we will discuss here is based on the more conventional shell model of these nuclei in which an inert ^{16}O core is assumed, and the $0d_{5/2}$, $1s_{1/2}$, and $0d_{3/2}$ orbits are active in the model space. The two-body effective interaction we use for this calculation is the realistic interaction designed by Kuo[7] for this mass region. For the eigenvalues of the diagonal one-body operator we use the observed energies of the lowest $\frac{5}{2}^+$, $\frac{1}{2}^+$, and $\frac{3}{2}^+$ states in ^{17}O. The results for this model which are discussed here are taken from a detailed study[1] of ^{16}O-core shell-model calculations for s-d-shell nuclei reported previously. We will sometimes refer to this calculation as K-dsd.

Most of the matrix elements used in these three calculations are listed in Table I. For the Kuo interaction used in the K-dsd calculations we list only those matrix elements which involve the $d_{5/2}$ and $s_{1/2}$ orbits. Over-all, the character of the Z-pds and F-pds interactions are similar, but there are significant differences in some individual matrix elements. Perhaps the most striking difference is for the diagonal matrix element involving the $|d_{5/2}{}^2, J=1^+, T=0\rangle$ state. In Z-pds this matrix element is 0, while in F-pds it has a value of about 2 MeV. In the conventional s-d shell-model calculation the largest component in the ^{18}F 1^+, $T=0$ ground state is $|d_{5/2}, d_{3/2}1^+, 0\rangle$. Since we omit the $d_{3/2}$ orbit from the active model space, such a state is not present in the pds calculations. In these calculations we introduce contributions of states involving $d_{3/2}$ particles by perturbative renormalization of matrix elements in the active space. It would not be surprising if there were some difficulties in attempting to introduce as a perturbation the effects of a component which is dominant in a given state. The discrepancy between these two matrix elements might be symptomatic of such a difficulty. The largest discrepancies between matrix elements of the interactions Z-pds and F-pds occur for the $T=0$ matrix elements. We have found in almost all instances in which we have searched for effective interactions that the $T=1$ matrix elements are determined with much smaller uncertainties than are the $T=0$ matrix elements, and this is also the case here.

We have included results for the two different interactions in the pds model to illustrate which properties of the calculated results are sensitive to the effective interaction. As we will show below, the results calculated with the two different interactions are not in general very different, and one interaction is not clearly superior to the other. We have included the conventional shell-model calculations so that we can see which states might be described as "core excited," and which states are sensitive to the presence or absence of the $d_{3/2}$ orbit. The calculations have all been made with the use of the Oak Ridge–Rochester shell-model computer programs.[8]

III. DISCUSSION OF RESULTS FOR ENERGY LEVELS AND SPECTROSCOPIC FACTORS

In this section we present the results of calculations of energy levels of ^{18}O, ^{18}F, ^{19}O, ^{19}F, ^{20}O, ^{20}F, and ^{20}Ne, in terms of the models described in the previous sections. We have also calculated spectroscopic factors for single-nucleon transfer reactions in which these nuclei are targets and/or residual nuclei.

A. $A=18$, $T=0$ (^{18}F)

The calculated and observed[9] spectra of excited states in ^{18}F are shown in Fig. 1 and listed in Table II. In the K-dsd shell-model spectrum, seven states are calculated to come below about 4 MeV excitation. There are reasonable partners for all of these states in the experimentally observed spectrum. In addition there is a 1^+, a 2^+, and two possible 3^+, $T=0$ states experimentally observed in the first 4 MeV of excitation which are *not* accounted for by the ^{16}O-core model, as well as four negative-parity states which, of course, cannot even be described in principle by a model with only positive-parity orbits. Both the positive- and negative-parity states not accounted for by the K-dsd calculations are present in the pds-model calculations. In both the Z-pds and F-pds calculated spectra there are more states calculated below 4 MeV than are found in the experimental spectrum. Neither one of the calculated pds spectra is obviously superior to the other.

The S factors extracted from the data on the

$^{17}O(^3He, d)^{18}F$ reaction[10] are presented in Table II together with the S factors calculated in the three models under discussion. For transitions to the lowest 1^+, 3^+, and 5^+, $T=0$ states, there is fair agreement between theory and extracted S factors. For the ground-state transition, the experimental number is significantly larger than either of the *pds* values. The *K-dsd* model predicts a significant $d_{3/2}$ admixture in this ground-state wave functions, but, of course, neither of the *pds* models include this orbit in the active space. As we discussed above, compensation is made for the omission of this orbit by a renormalization of the two-body interaction. The calculated results we will discuss here suggest that in the *Z-pds* calculation, the $s_{1/2}$ admixtures are enhanced over those in the ^{16}O-core model for the low-lying states of ^{18}F while $d_{5/2}$ admixtures are more enhanced in the *F-pds* calculations. (See the S factors calculated for transitions to the lowest 1^+, $T=0$ and 3^+, $T=0$ states.) The major discrepancy between the *pds*-model results and the stripping data concerns the 2^+, $T=0$ state observed at 2.52 MeV. The first possible model counterpart for this level is calculated to have a higher excitation energy than this in both *pds* models and, more importantly, is predicted to have a large S factor, while no such strength is observed for the 2.52-MeV level. The calculated strengths for the $^{19}F(p, d)^{18}F$ reaction are summarized in Table II. Results for this experiment have not been reported so far.

In summary, the core-excited model seems to give a reasonable accounting for the states in ^{18}F which do not fall within the province of the ^{16}O-core model with the exception of the 2^+, $T=0$ level observed at 2.52 MeV, which appears to have a quite different wave function from the lowest *pds* model 2^+, $T=0$, which occurs at a higher excitation energy.

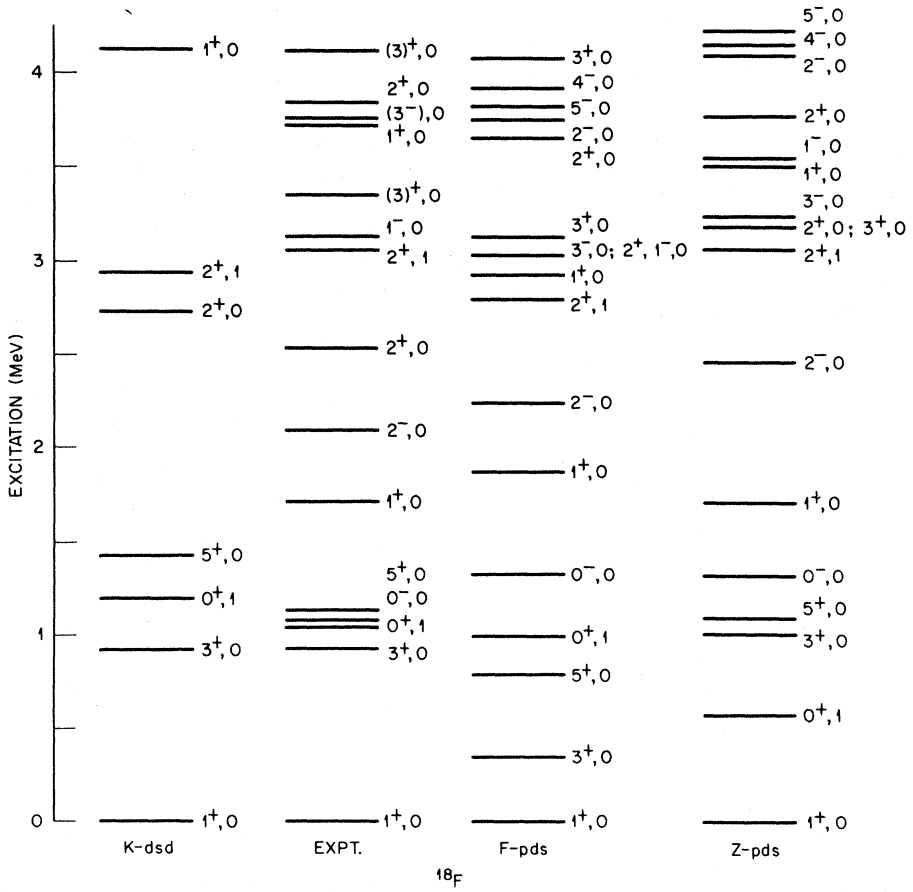

FIG. 1. Calculated and observed (Ref. 9) energies of low-lying states in ^{18}F. The captions *K-dsd*, *F-pds*, and *Z-pds* are related to the model space and interaction used to calculate the given spectra as explained in the text.

TABLE II. Excitation energies and spectroscopic factors for $A=18$, $T=0$ system.

					S factor $^{17}O \rightarrow A=18$, $T=0$					S factor $^{19}F \rightarrow A=18$, $T=0$		
		Energies (MeV)			Expt.[b]	*K-dsd*	*Z-pds*	*F-pds*				
J^π	Expt.[a]	*K-dsd*	*Z-pds*	*F-pds*	$l=2/l=0$	$l=2/l=0$	$l=2/l=0$	$l=2/l=0$	l	*K-dsd*	*Z-pds*	*F-pds*
1^+	0	0	0	0	1.5/0	1.1/0	0.6/0	0.9/0	0	0.4	0.6	0.5
1^+	1.70		1.71	1.87			0/0	0/0	0		0	0
1^+	3.72	4.13	3.51	2.92		0.5/0	0/0	0.1/0	0	0	0	0
2^+	2.52	2.72	3.18	3.03		0.3/0.5	0/0.4	0/0.5	2	0.3	0.1	0.2
2^+	3.84	6.88	3.79	3.65	<1.1/1.0	0.6/0.3	0/0.5	0/0.4	2		0	0
3^+	0.94	0.92	1.01	0.32	<0.7/0.6	0.6/0.8	0.6/0.6	0.8/0.5	2	0.7	0.8	0.9
3^+	(3.36)		3.16	3.12	0/0		0/0	0/0	2		0	0
3^+	4.12	4.87	4.08	4.08	1.5/0.3	1.3/0.3	0.7/0.1	0.7/0.3	2	0	0	0.1
5^+	1.13	1.12	1.09	0.78	2.0/0	2.0/0	1.8/0	1.8/0				
0^-	1.09		1.33	1.32					1		0.2	0.2
1^-	3.13		3.55	3.03					1		0.6	0.5
2^-	2.10		2.46	2.23			0.1	0.1				
3^-	3.78		3.23	3.03			0.2	0.1				

[a] Reference 9.
[b] Reference 10.

TABLE III. Excitation energies and S factors for $A=18$, $T=1$ system.

					S factor $^{17}O \rightarrow A=18$, $T=1$						S factor $^{19}F \rightarrow A=18$, $T=1$		
		Energies (MeV)			Expt.[b]	*K-dsd*	*Z-pds*	*F-pds*		Expt.[c]	*K-dsd*	*Z-pds*	*F-pds*
J^π	Expt.[a]	*K-dsd*	*Z-pds*	*F-pds*	$l=2/l=0$	$l=2/l=0$	$l=2/l=0$	$l=2/l=0$	l				
0^+	0	0	0	0	2.3/0	1.7/0	1.6/0	1.6/0	0	0.6	0.5	0.6	0.5
0^+	3.63	4.03	3.84	3.70	(0.2)/0	0.2/0	0.5/0	0.5/0	0	0.1	0	0	0
0^+	5.33	14.39	5.04	5.01	(<0.2)/0		0/0	0/0	0	0.2		0.2	0.2
1^+		8.85	9.40	8.99									
1^+		10.08	10.91	10.73									
2^+	1.98	1.74	2.50	1.80	1.5/0.3	1.1/0.4	0.8/0.4	0.7/0.5	2	0.8	0.6	0.4	0.5
2^+	3.92	3.99	4.39	4.18	1.0/0.4	0.9/0.6	1.0/0.4	1.1/0.3	2	0.0	0.1	0	0
2^+	5.25	8.42	5.85	5.10	0/(0.3)		0/0	0/0.2	2	0.5		0.4	0.4
3^+	5.37	4.94	5.97	6.34	0/0.1	0/1.0	0/0.9	0/0.9		0	0	0	0
4^+	3.55	3.38	4.62	3.89	2.0/0	1.9/0	1.8/0	1.8/0					
4^+		7.79	7.77	7.05									
0^-	(6.86)		5.85	5.99								0.6	0.6
1^-	4.45		4.04	4.16					1	2.0		1.8	1.5
1^-	(6.19)		6.44	6.26									0.2
2^-	(5.52)		5.97	5.08			0.1	0					
2^-			6.74	5.90			0.1	0					
3^-	5.09		4.61	4.89			0.2	0					
3^-			6.45	6.09			0	0.1					
4^-			7.71	6.94									

[a] Reference 9.
[b] Reference 11.
[c] Reference 12.

B. $A = 18$, $T = 1$

In Fig. 2, the experimentally observed[9] spectrum of ^{18}O is shown together with the three sets of shell-model results. In this system, there are $J = 0^+$ and $J = 2^+$ states below 6 MeV unaccounted for in the ^{16}O-core model, as well as at least three negative-parity states. Here, the *pds* results look to be in quite good agreement with experiment, with the *F-pds* results showing somewhat better quantitative agreement. There are obvious calculated analogs for all states observed in ^{18}O below 6 MeV. The *pds* results are similarly gratifying for predicted *S* factors. In Table III, these values are compared to values extracted from a study of the ^{17}O$(d,p)^{18}$O reaction.[11] For these data, the *Z-pds* results appear better than the *F-pds* results, mainly because of the distribution of strengths between $l = 0$ and $l = 2$ transitions to the lowest two 2^+ states. A similar evaluation holds for the ^{19}F$(d,{}^3\text{He})^{18}$O reaction.[12] The pickup strength to the 1^- state at 4.45 relates to the degree of occupation of the $0p_{1/2}$ orbit. The observed strength suggests the $p_{1/2}$ shell is essentially full. Both calculated values are smaller than the experimental number, which could indicate that the *pds* models overestimate the degree of excitation, *F-pds* to a greater extent than *Z-pds*. This matter will be discussed at greater length below.

C. $A = 19$, $T = \frac{1}{2}$

The observed[9] and calculated spectra of the $A = 19$, $T = \frac{1}{2}$ system are presented in Table IV and in Fig. 3. The experimental and theoretical values of the *S* factors for the population of these states by stripping[13] from ^{18}O and pickup[12] from ^{20}Ne are also presented in Table IV. There are at least 21 states observed below 6 MeV in this system, eight of which probably have negative parity. In this same energy region, the *K-dsd* results account for seven levels, and put three more states between 6 and 7 MeV which might

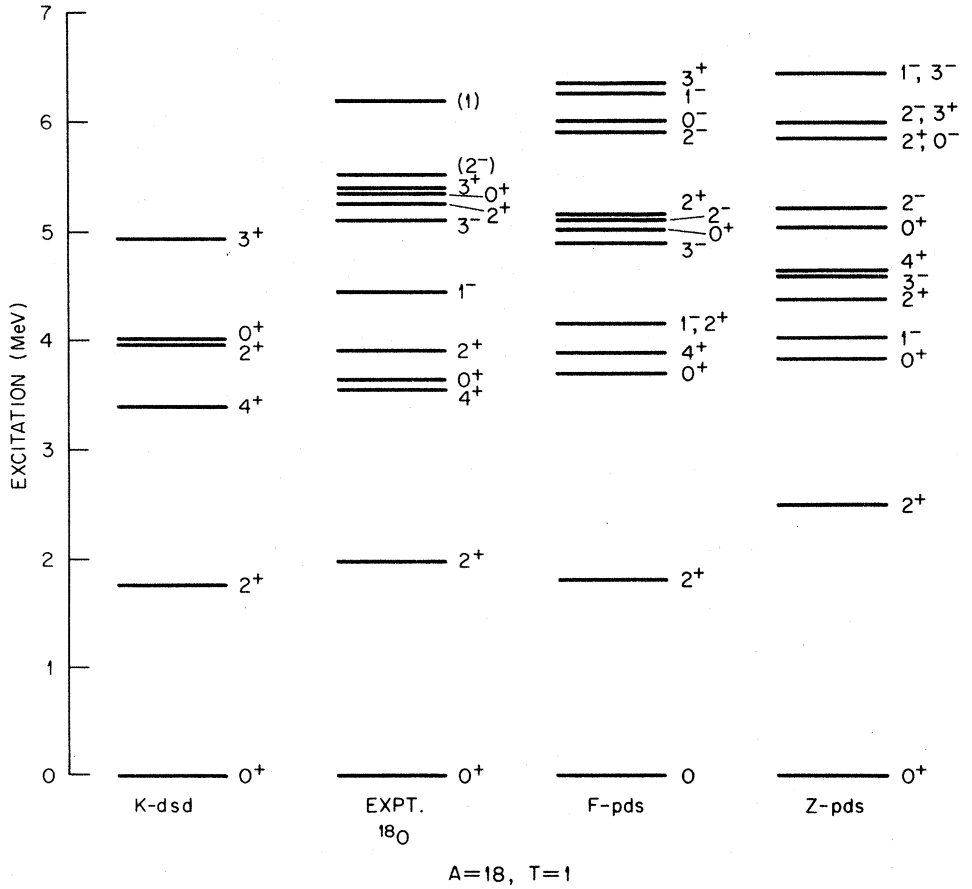

FIG. 2. Calculated and observed (Ref. 9) energies of low-lying states in ^{18}O. The captions *K-dsd*, *F-pds*, and *Z-pds* are related to the model space and interaction used to calculate the given spectra as explained in the text.

correspond to levels which occur around 6 MeV experimentally. All of these ^{16}O-core states can be correlated with levels in the observed spectrum. The total number and density of levels in the spectra calculated in the *pds* models are in general agreement with experiment. It was pointed out in the Introduction that ^{19}F showed essentially degenerate positive- and negative-parity $K=\frac{1}{2}$ bands. We see that this feature is accounted for in both *pds* models. The major discrepancy between the *pds* and experimental spectra in the region of low excitation energies concerns the first $\frac{3}{2}^+$ level. The lowest $\frac{3}{2}^+$ level observed experimentally come significantly below the energies of the lowest $\frac{3}{2}^+$ states in the *pds* spectra. On the other hand, the ^{16}O-core calculation puts the first $\frac{3}{2}^+$ state at the correct energy. As is discussed below, the $\frac{3}{2}^+$ state experimentally observed at 1.56 MeV has a significant single-particle strength for stripping from ^{18}O. This implies that this state contains a significant $d_{3/2}$ component and hence it should be difficult to account for this level in a model in which the $d_{3/2}$ orbit is omitted. The fact that even the results of the searched interaction fail to put the first $\frac{3}{2}^+$ state low enough is consistent with this idea, and, in fact, the level should probably not have been included in the set of data from which the empirical interaction was determined. However, the search was retried without this state included in the set of levels to be fitted, and the over-all results were not significantly altered. This indicates that the effects of renormalization of the interaction for the basis space truncation arise from the more general trends of the entire data set.

Levels in $A=19$, $T=\frac{1}{2}$ can be populated by proton transfer reactions from ^{20}Ne and ^{18}O and by neutron pickup from ^{20}Ne. Four states are populated strongly in the proton stripping reaction. For transitions to the first $\frac{1}{2}^+$ and first $\frac{5}{2}^+$ states, the strength calculated in all three models are consistent with experiment. The transition to the $\frac{3}{2}^+$ state at 1.56 MeV, which indicates a significant admixture of $d_{3/2}$ single-particle strength in this

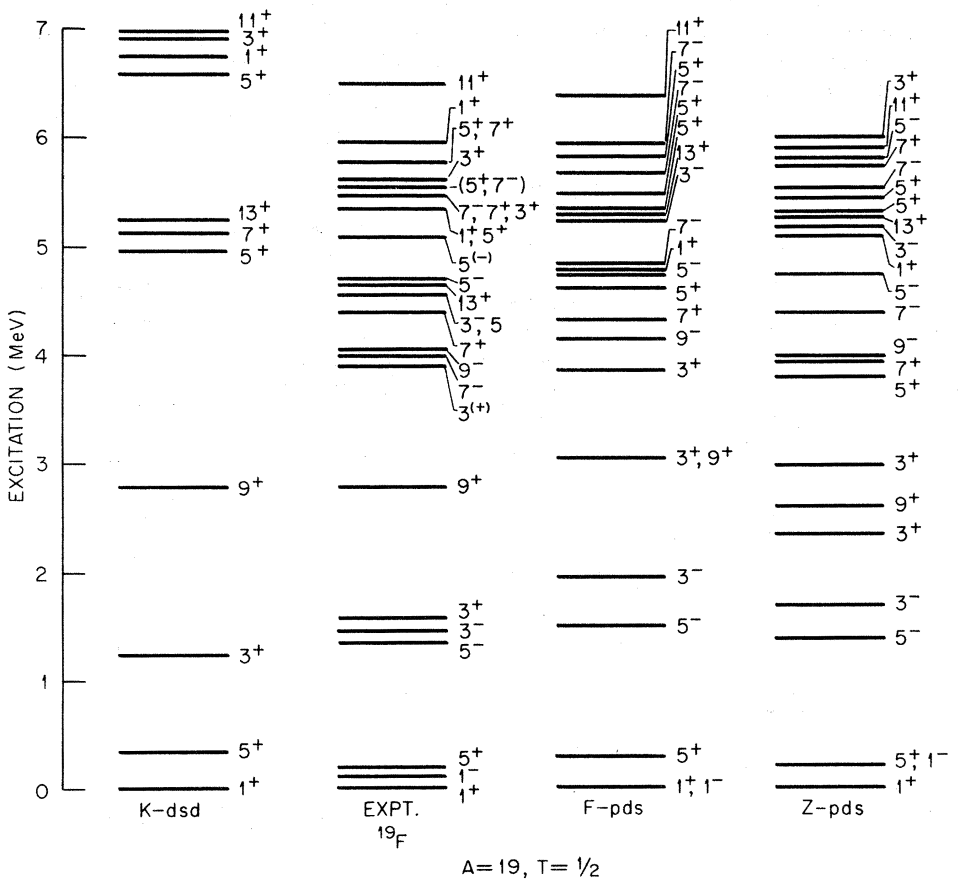

FIG. 3. Calculated and observed (Ref. 9) energies of low-lying states in ^{19}F. The captions *K-dsd*, *F-pds*, and *Z-pds* are related to the model space and interaction used to calculate the given spectra as explained in the text.

state, is reproduced in the *K-dsd* calculation. As already discussed, this orbit is not present in our *pds* models, so the observed transition to the 1.56 MeV cannot be reproduced even in principle.

The strength of the stripping transition to the $\frac{1}{2}^-$ state at 110 keV is related to the amount of *p*-shell core excitation, as was the $^{19}F \rightarrow A = 18$ pickup data to the 1^- state. This transition is forbidden if the $p_{1/2}$ shell is filled and if we can ignore higher $\frac{1}{2}^-$ single-particle orbits. The *pds* models predict more than twice as much strength as is quoted from experiment, which suggests again that the models predict too much core excitation. (There is always the possibility that the extracted number might be in error due to uncertainties in the reaction analysis.)

Similar results are obtained from examination of the pickup reactions leading from the ^{20}Ne ground state to excited states in $A = 19$, $T = \frac{1}{2}$. There is a strong transition observed[12] to the first $\frac{3}{2}^+$ state of ^{19}F in $^{20}Ne(d, {}^3He)^{19}F$. This is reproduced by the ^{16}O-core model, but not, of course, by the *pds* models. Comparison of the predicted and observed transition strengths to the lowest $\frac{1}{2}^-$ state again seems to imply that the models contain too much core excitation. The excitation of the $\frac{3}{2}^-$ state at 1.51 MeV is forbidden in all the models.

D. $A = 19$, $T = \frac{3}{2}$

The calculated and observed[9] ^{19}O levels for $A = 19$, $T = \frac{3}{2}$ are shown in Fig. 4 and, together with the calculated and observed[14] *S* factors for the $^{18}O \rightarrow {}^{19}O$ reaction, are presented in Table V.

The *K-dsd* spectrum is not in particularly good agreement with the experimental data available. The first $\frac{1}{2}^+$ level is too low by 1 MeV, as is the second $\frac{5}{2}^+$ state. The *pds* spectra are similarly in only qualitative agreement with experiment. In none of the models is there a second $\frac{1}{2}^+$ state to correlate with the state observed at 3.24 MeV. (In point of fact, the data on the transition to this state do not suggest a very convincing $\frac{1}{2}^+$ assignment.) Both *pds* models predict the $\frac{1}{2}^-$ and $\frac{3}{2}^-$ levels too low by an MeV. The predicted *S* factors for $^{18}O \rightarrow {}^{19}O$ transition are consistent with the rather sparse data.[14]

E. $A = 20$, $T = 0$

The structure of ^{20}Ne has been the subject of numerous theoretical and experimental investigations. Much of this interest has been stimulated by the apparent rotational nature of the structure of this nucleus. Since ^{20}Ne can be discussed in terms of fairly complete microscopic calculations, it is an obvious meeting ground for

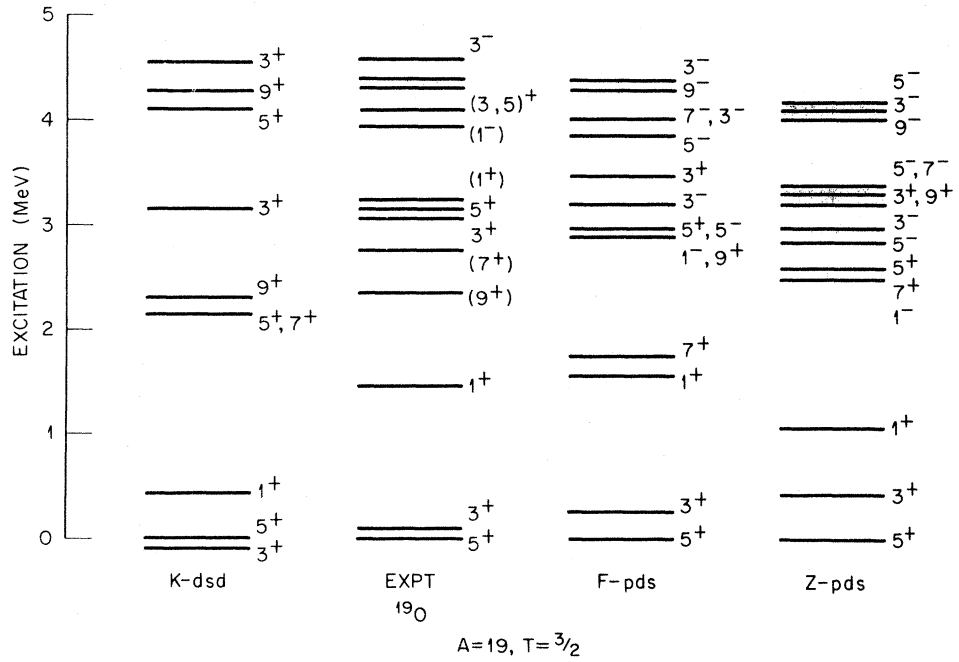

FIG. 4. Calculated and observed (Ref. 9) energies of low-lying states in ^{19}O. The captions *K-dsd*, *F-pds*, and *Z-pds* are related to the model space and interaction used to calculate the given spectra as explained in the text.

collective and microscopic models. For this reason we will discuss this spectrum in some detail. In Fig. 5, the observed spectrum[9] is shown as are the spectra calculated in the three models. The observed spectrum shows many more levels in the energy region below 10 MeV than are obtained in the *K-dsd* calculation. The *pds* models, on the other hand, do an excellent job of accounting for these extra states. The *Z-pds* spectrum is generally too expanded with respect to the observed spectrum, but, over-all, there is little qualitative difference between the two calculated *pds* spectra, and there is a remarkable qualitative similarity of the calculated spectra with the observed ones which becomes more apparent in Fig. 6, as we now discuss.

In Fig. 6, there are 24 levels below about 10 MeV, 17 of which are generally ascribed[15] to five rotational bands, with K^π values of 0^+, 0^+, 0^+, 0^-, and 2^-. Such a decomposition of the observed spectrum is shown in the lower half of Fig. 6. In the *F-pds* calculation, there are 21 levels below about 10 MeV. 17 of these levels can be placed in five rotational bands with K^+ values of

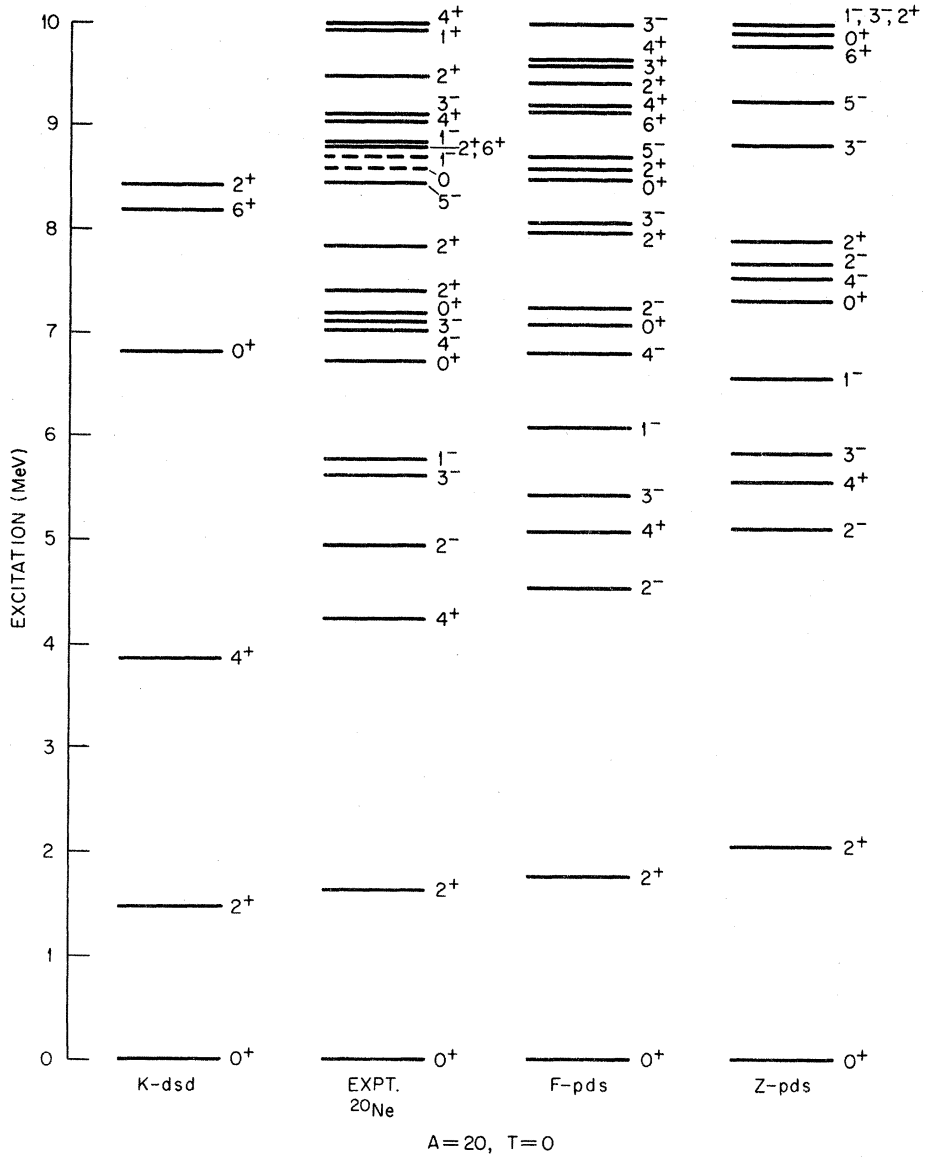

FIG. 5. Calculated and observed (Ref. 9) energies of low-lying states in ^{20}Ne. The captions *K-dsd*, *F-pds*, and *Z-pds* are related to the model space and interaction used to calculate the given spectra as explained in the text.

0^+, 0^+, 0^+, 1^-, and 2^-. In decomposing the calculated spectrum, we have put each successive level of a given spin in the lowest possible band; i.e., the second $J^\pi = 2^+$ state is in the second $K = 0^+$ band, the third $J^\pi = 4^+$ state is in the third $K = 0^+$ band, etc. (This is not the case in the experimental spectrum. There, the cluster-transfer data suggest[16] that the third $J^\pi = 4^+$ state is in the second $K = 0^+$ band and the second $J^\pi = 4^+$ state is in the third $K = 0^+$ band.) The excitation energy of the observed band-head state is indicated in the calculated spectrum by a dashed line. The similarity of these two plots is striking.

In the calculated spectrum in Fig. 6 below 10 MeV, three of the four states not assigned to the first "bands" are $J^\pi = 2^+$, 3^+, and 4^+, suggesting a $K = 2^+$ band. In the model, this is a 6p-2h band (on grounds described below). It could be analogous to the low-lying $K = 2^+$ band seen in ^{22}Ne.[1] In the observed spectrum, two of the three positive-parity states not included so far in some bands are $J^\pi = 2^+$ states, and one of these could be the band head of the $K^\pi = 2^+$ band.

One interpretation[16] of the cluster-transfer data says that the first two $K = 0^+$ bands consist primarily of states with 4p in the s-d shell, and the third $K^\pi = 0^+$ band has an 8p-4h character. From an analysis of occupation probabilities, discussed below, we find that the third $K^\pi = 0^+$ band has essentially a 6p-2h character, in contradiction to the interpretation of the cluster data.

We have not mentioned an obvious discrepancy between the calculated and observed spectra shown in Fig. 6. In the observed spectrum, the second negative-parity band consists of states with $J^\pi = 1^-$, 3^-, and 5^-. The 4p and 8p transfer data[16] suggest that this band is a $K = 0^-$ band, from the configuration $(sd)^3(fp)^1$. The models used here

TABLE IV. Excitation energies and spectroscopic factors for $A = 19$, $T = 1/2$ system.

	Energies (MeV)				S factors for ^{18}O$\rightarrow A=19$, $T=\frac{1}{2}$					S factor for ^{20}Ne$\rightarrow A=19$, $T=\frac{1}{2}$				
$2J^\pi$	Expt.[a]	K-dsd	Z-pds	F-pds	l	Expt.[b]	K-dsd	Z-pds	F-pds	l	Expt.[c]	K-dsd	Z-pds	F-pds
1^+	0	0	0	0	0	0.5	0.5	0.6	0.5	0				
1^+	5.34	6.75	4.79	5.09	0	0.1	0	0	0	0	1.5	0.9	1.4	1.3
1^+	6.25	8.04	6.07	6.21	0			0		0		0	0	0
3^+	1.57	1.25	3.05	2.35	2	0.4	0.3				1.0	0.7		
3^+	3.91		3.86	2.98								0		
3^+	5.50	6.45	5.95	5.97			0							
3^+		6.93	6.72	6.76										
5^+	0.20	0.36	0.27	0.24	2	0.6	0.7	0.6	0.6		3.4	2.3	2.9	3.2
5^+	4.50	4.97	4.62	3.80	2		0.1	0.1	0.1			0	0.3	0.3
5^+		6.59	5.35	5.30	2		0	0	0			0	0	0
5^+		7.72	5.50	5.45	2			0	0				0	0
7^+	4.38	5.12	4.35	3.94										
7^+	5.47	5.68	5.83	5.74										
7^+		6.76	6.24	6.17										
9^+	2.79	2.78	3.06	2.59										
11^+	6.50	6.98	6.35	5.90										
13^+	4.65	5.26	5.30	5.26										
1^-	0.11		0	0.23	1	0.2		0.4	0.4		3.7		3.2	2.8
3^-	1.51		1.95	1.70							0.9			
3^-	4.56		5.23	5.17										
5^-	1.35		1.51	1.42										
5^-	4.68		4.73	4.74										
5^-			5.86	5.82										
7^-	4.00		4.85	4.39										
7^-	5.43		5.66	5.53										
7^-			6.66	6.50										
9^-	4.03		4.15	4.00										

[a] Reference 9.
[b] Reference 13.
[c] Reference 12.

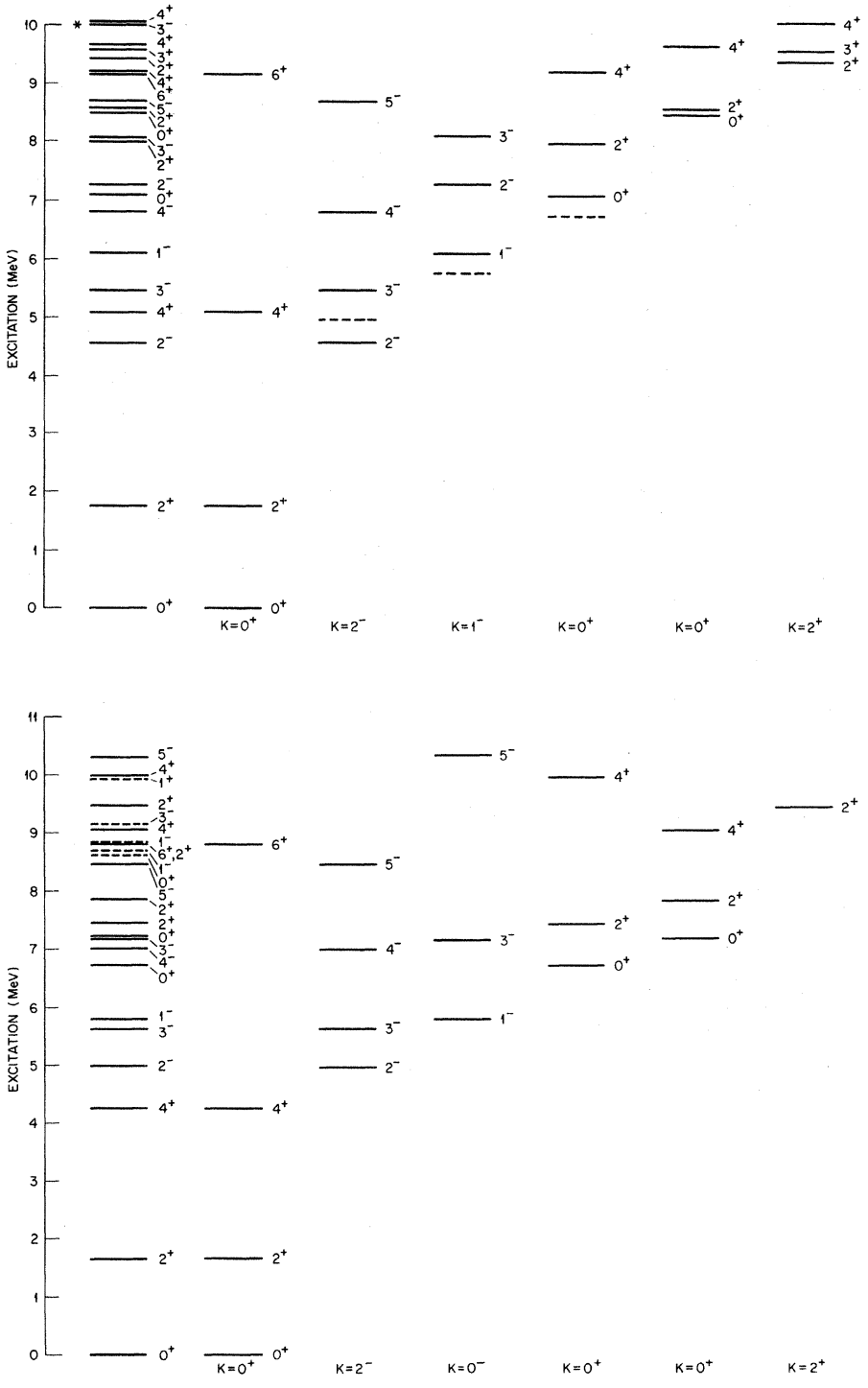

FIG. 6. Decomposition of observed and calculated spectra of ^{20}Ne into rotational bands. The upper spectrum is the spectrum calculated with the *F-pds* interaction, and the lower spectrum is the observed one. In the calculated spectrum, the dashed lines indicate the experimentally observed position of the band-head state for each band.

do not include such configurations. In the calculated spectrum, the second negative-parity band consists of states with $J^\pi = 1^-$, 2^-, 3^-, etc., and is most likely a 5p-1h $K = 1^-$ band. In the observed spectrum, the extra negative-parity states are $J^\pi = 1^-$, 1^-, and 3^- states. Two of these states could be members of a $K^\pi = 1^-$ band of a 5p-1h character. They are at a significantly higher energy than the calculated $K = 1^-$ band. However, the lowest SU(3) state of a 5p-1h character which contains a $K = 1^-$ band is known to have a large component with a spurious center-of-mass motion. (This was pointed out to us by A. Arima.) This suggests that the shell-model $K = 1^-$ band may be similarly contaminated. If the states in the observed spectrum around 9 MeV are members of this $K = 1^-$ band, it suggests the possible existence of a $J^\pi = 2^-$ state in this same energy region.

There is considerable interest in the shape of the line which plots the energy versus $J(J+1)$ for the states of an assumed rotational band. We have made such plots from the known experimental levels of ^{20}Ne for the three $K = 0^+$ bands and the $K = 2^-$ band, and for all calculated states up to the highest spin possible in our model space ($J = 10^+$ and $J = 9^-$) in Fig. 7. The qualitative features of these curves are similar in both calculations, in that they both "kink" at the same points and in the same direction. We include the 10^+ state in the plot of the ground-state band, although it is questionable to do so. The question of the "cutoff" of this band at the 8^+ state in ^{20}Ne has been discussed in some detail elsewhere.[17] In our model space, the 10^+ has at least two $p_{1/2}$ holes, while the remaining members of the band are dominated by four s-d-shell particles outside the close $p_{1/2}{}^4$ configuration. To lowest order, there is no one-body $E2$ transition between these states, and the calculated $E2$ transition for the 10^+ to 8^+ transition is very weak. In the usual operational definition of a rotational band, i.e., that $E_J \propto J(J+1)$ and the $B(E2)$ value for the transition from $J \to J-2$ is strong, the 10^+ is not a member of the rotational band. The theoretical curves bend upward significantly more rapidly between the 8^+ and the 10^+ state. A possible reason for this is that there are only two 10^+ states in our model space, so there is no coherent collective effect possible which would depress the energy of this state as there is for the lower spin states. Pittel[17] suggests that admixing some one-particle 2 $\hbar\omega$ excitations in this state could lead to significant $E2$ strength and such admixtures would quite likely depress the excitation energy of the state.

For the second and third $K = 0^+$ bands, we have accepted the assignments suggested by the cluster-transfer experiments. If they are correct, the

TABLE V. Energies and spectroscopic factors for $A = 19$, $T = \frac{3}{2}$ system.

	Energies (MeV)					S factors ^{18}O$\to A = 19$, $T = \frac{3}{2}$			
$2J^\pi$	Expt.[a]	K-dsd	Z-pds	F-pds	l	Expt.[b]	K-dsd	Z-pds	F-pds
1^+	1.47	0.44	1.07	1.57	0	0.5	0.9	0.7	0.7
1^+	(3.24)	5.54	6.43	5.91	0			0	0
3^+	0.10	−0.12	0.44	0.26	2	0	0		
3^+	(3.07)	3.14	3.32	3.49			0.1		
3^+		4.53	4.77	4.38			0.8		
5^+	0	0	0	0	2	0.4	0.7	0.6	0.6
5^+	3.15	2.15	2.85	2.94	2	weak	0	0	0
5^+	(4.12)	4.11	4.83	4.98			0	0	0
7^+	(2.78)	2.17	2.58	1.72					
9^+	(2.37)	2.29	3.32	2.90					
1^-	(3.95)		2.50	2.90	1	strong		c	0.2
3^-	4.58		3.22	3.22					
3^-			4.12	4.03					
5^-			3.00	2.95					
5^-			2.40	3.88					
7^-			3.40	4.01					
9^-			4.02	4.29					

[a] Reference 9.
[b] Reference 14.
[c] Number not calculated.

second 0^+ band shows no obvious qualitative deviation from a straight line, and this is reproduced qualitatively by both interactions. The third $K=0^+$ band shows a definite upward bend with increasing J, and this feature is reproduced by both calculations. For the second and third $K=0^+$ bands, the Z-pds model is in somewhat better agreement with the experimental trends of these curves.

For the $K=2^-$ band, the observed deviations from a pure $J(J+1)$ dependence are relatively small, and this is the feature observed in both calculations up to the 8^- state. There is a pronounced kink between the 8^- and 9^- states. This again may be a truncation effect.

Thus, the calculated energy levels very obviously display the rotational characteristics which have been ascribed to the experimental levels, and they also display deviations from the rigid rotor predictions very similar to those exhibited by the observed levels.

In Table VI, calculated and experimentally[18] determined spectroscopic factors for proton stripping from ^{19}F and ^{20}Ne are presented. Within the accuracy of the experimental numbers, the conventional shell-model results are in excellent agreement with the experimental numbers. The calculated numbers in the two core-excited models are quite similar to each other. The strength for the $d_{5/2}$ transition to the ground state is more than twice as big as the extracted number. This implies that the renormalized numbers are overemphasizing the $d_{5/2}$ admixtures in these wave functions. The calculated values for transitions to the remaining states are in good qualitative agreement with experiment.

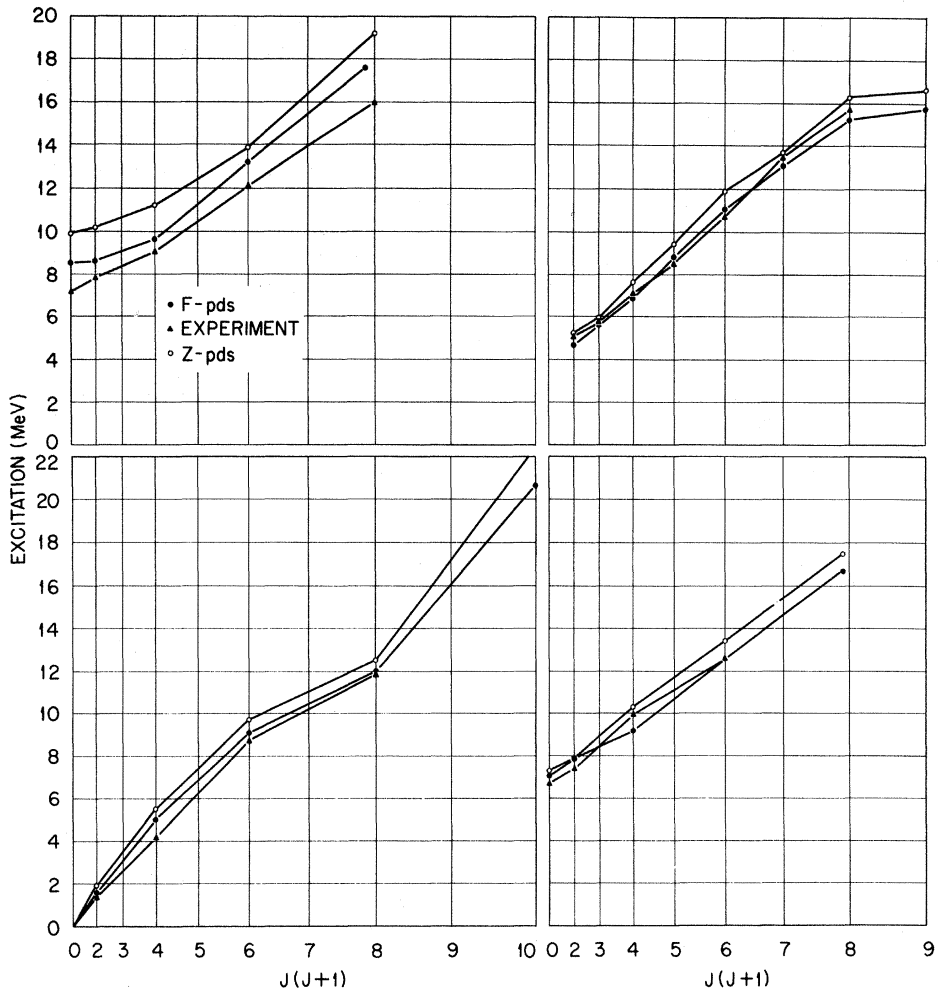

FIG. 7. Plots of E_J versus $J(J+1)$ for members of rotational bands in ^{20}Ne. The lower left-hand plot is for the ground-state band, the lower right-hand plot is for the first excited "$(sd)^4$" band, the upper left-hand plot is the second excited "deformed" band, and the upper right-hand plot is the $K=2^-$ band.

F. $A = 20$, $T = 1$

The calculated and observed[9] spectra of ^{20}F are shown in Fig. 8. The excitation energies and spectroscopic factor for the ^{19}F$(d,p)^{20}$F reaction[19] are presented in Table VII. In the observed spectrum, there are 13 states below 3 MeV, 8 positive-parity and 5 negative-parity states. All the calculated spectra show more positive-parity levels than this. The trend seems to be that the higher excited states come too low in energy. But there are good analogs to the observed positive-parity states in all three calculated spectra, and the states appear in roughly the right order. The simplest Nilsson model would predict low-lying $K = 1^+$, 2^+, 1^-, and 2^- bands, and states which could be ascribed to such bands account for all the observed levels below 3 MeV. However, the level spacing of these "bands" are significantly distorted from a $J(J+1)$ spectrum. There are no significant qualitative differences between the spectra calculated in the *Z-pds* and *F-pds* models.

Calculated spectroscopic factors and factors extracted from experimental[19] data for the ^{19}F-$(d,p)^{20}$F reaction are presented in Table VII. (These numbers were not calculated for the *Z-pds* interaction.) For the positive-parity states, the *K-dsd* and *F-pds* results are quite similar and in acceptable agreement with experiment. The data imply more splitting of the various single-particle strengths than the *K-dsd* results show, and generally this splitting is reproduced by the *F-pds* calculation. The most obvious discrepancy for the positive-parity states is that the $s_{1/2}$ strength is too low by 0.5 to 1.0 MeV in both calculations.

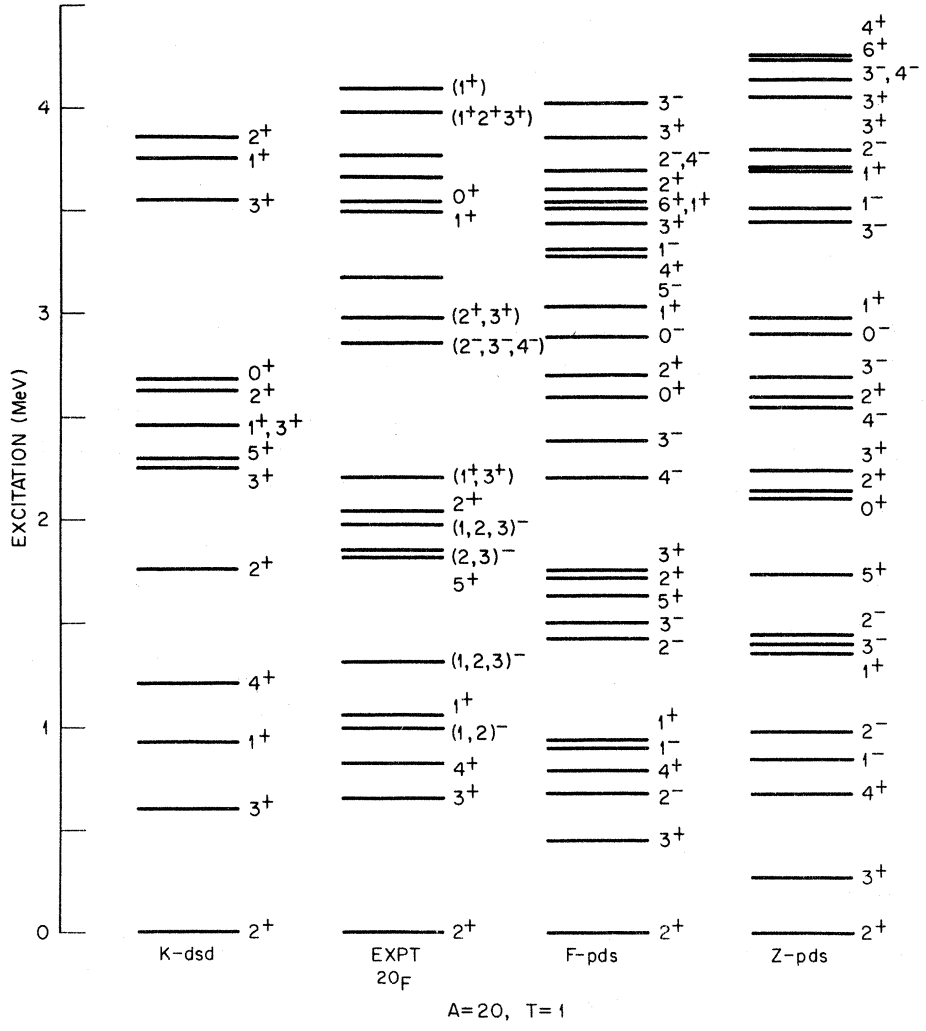

FIG. 8. Calculated and observed (Ref. 9) energies of low-lying states in ^{20}F. The captions *K-dsd*, *F-pds*, and *Z-pds* are related to the model space and interaction used to calculate the given spectra as explained in the text.

No negative-parity states are significantly populated in the (d,p) reaction and no significant strengths are predicted for such transitions.

G. $A=20$, $T=2$

The calculated and observed[9] spectra for the $A=20$, $T=2$ system are shown in Fig. 9. There are no single-particle transfer reactions possible which populate states in this system, and there are relatively few other data available. For the spectra shown in Fig. 9, we see that these two core-excited model calculations are seemingly in better agreement with experiment than in the *K-dsd* calculation, the main difference being that the excited 0^+ is calculated to be at the correct energy in *Z-pds* and *F-pds*.

IV. PARTICLE-HOLE DESCRIPTION OF STATES IN $\hat{A}=18$, 19, AND 20

In this section, we attempt to describe the wave functions obtained in these calculations in a qualitative way, primarily as np, mh states. Zuker[4] has already presented a detailed analysis of the wave functions in the $A=18$ system. He has shown very clearly that the states which are described by the conventional shell model with an inert ^{16}O core can be similarly described in the core-excited calculations, if the term "inert ^{16}O core" is replaced by "the ground state of ^{16}O." In other words, the ground state of ^{18}F has a complicated structure in the spherical representation we use, but it is essentially a 1^+, $T=0$ state of 2p in the *s-d* shell coupled to the ground state of ^{16}O as calculated in the same core-excited model. The best analysis of our wave functions would be to make weak-coupling decompositions of the wave functions in terms of states coupled to states in the $A=15$, 16, and 17 nuclei. We have not done this, and here we merely attempt to obtain a qualitative description of the wave functions purely in terms of the expectation value of the $p_{1/2}$-number operator (which we will refer to as the $p_{1/2}$ occupation), which reflects the oc-

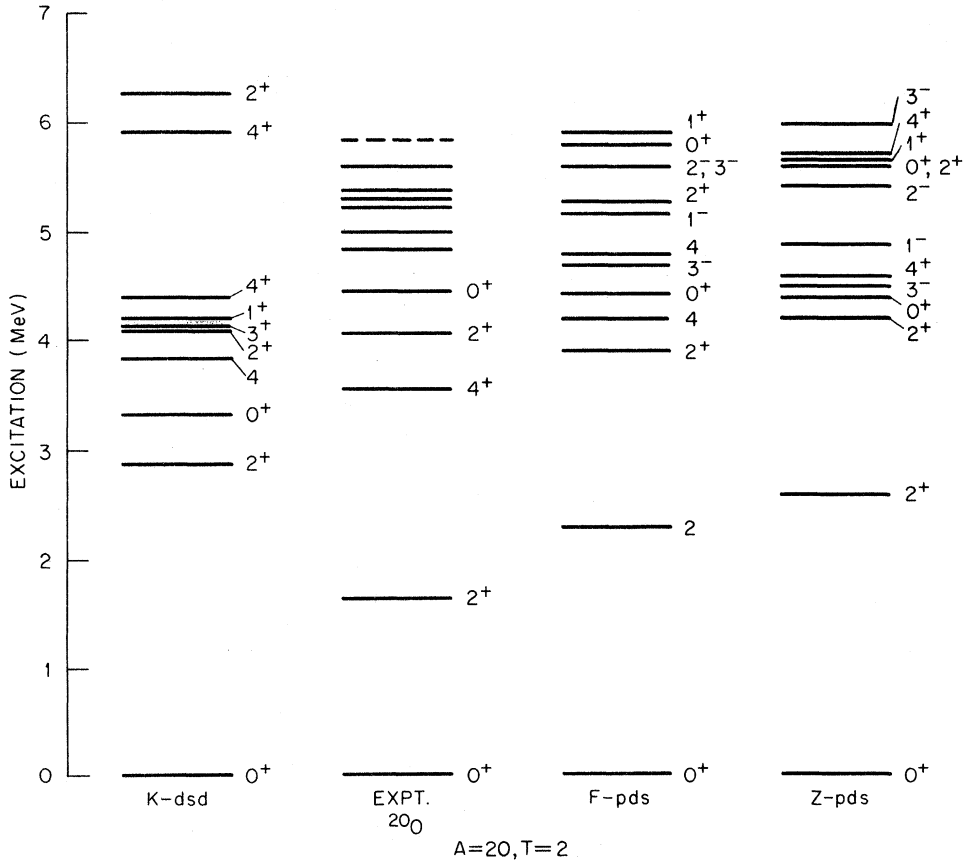

FIG. 9. Calculated and observed (Ref. 9) energies of low-lying states in ^{20}O. The captions *K-dsd*, *F-pds*, and *Z-pds* are related to the model space and interaction used to calculate the given spectra as explained in the text.

cupation of the $p_{1/2}$ orbit in each state. In the ^{16}O calculations, Zuker's interaction leads to a $p_{1/2}$ occupation of 3.20 for the ground state, while the fitted interaction gives a value of 3.26. In the first-excited 0^+ state in ^{16}O, these values are 0.42 and 0.47, respectively. This latter state is generally referred to as the 4p-4h state of ^{16}O. This suggests that states with $p_{1/2}$-occupation values around 3.2 might be described as 0h states, while states for which this value is around 0.5 are 4h states.

In Table VIII, the $p_{1/2}$ occupations for the ground states of the nuclei treated here are listed for both the *Z-pds* and *F-pds* interactions. Perhaps the most surprising point illustrated here is the relatively weak evidence for any Pauli blocking effect. One would expect that the probability for core-excitation would decrease as the number of particles already present in the orbits above the "core" increases. In our model, if there are 20 active particles outside ^{12}C, there is only one state, the $(p_{1/2}^4, d_{5/2}^{12}, s_{1/2}^4)$ configuration with all shells filled. There is no core excitation here because all orbits are filled. To lowest order in our calculation, there are no *s-d* particles in the ground state of ^{16}O, and there are four *s-d* particles in the ground state of ^{20}Ne, but the amount of core excitation is essentially identical for these two nuclei. The other systematic features shown here are that for states beyond ^{16}O, *F-pds* gives more core excitation than does *Z-pds*, and there is significantly more core excitation in the identical particle nuclei (^{18}O, ^{19}O, ^{20}O, or ^{18}Ne, ^{19}Na, ^{20}Mg).

As mentioned above, a detailed analysis of the mass-18 wave functions has already been made, so we will give only a brief description of these states. For the $T=0$ states in ^{18}F, the lowest

TABLE VI. Excitation energies and spectroscopic factors for $A=20$, $T=0$ system.

	Energy (MeV)				S factors for $^{19}\mathrm{F}\rightarrow A=20$, $T=0$ states				
J^π	Expt.[a]	*K-dsd*	*Z-pds*	*F-pds*	l	Expt.[b]	*K-dsd*	*Z-pds*	*F-pds*
0^+	0	0	0	0	0	0.6	0.9	1.4	1.3
0^+	6.72	6.81	7.33	7.09	0	0.9	1.0	1.0	0.8
0^+	7.20	12.81	9.92	8.49	0	<0.1	0	0	0
1^+	(9.95)	11.78	12.86	11.33	0				
2^+	1.63	1.46	2.05	1.74	2	1.3	1.0	0.9	0.9
2^+	7.42	8.43	7.91	7.98	2	0.3	0.2	0.2	0.2
2^+	7.83	10.37	10.17	8.57	2	0	0	0	0
3^+		10.69	10.07	9.58					
4^+	4.25	3.86	3.58	5.09					
4^+	9.04	10.18	10.27	9.19					
4^+	9.99	11.19	11.22	9.62					
5^+		12.48	12.39	11.64					
6^+	8.78	8.19	9.77	9.14					
6^+	12.15	13.41	13.54	12.57					
6^+	12.56	15.24	13.80	13.21					
8^+	11.95	12.36	12.48	11.98					
8^+		16.37	17.46	16.67					
8^+		22.77	19.13	17.54					
10^+			21.36	19.85					
0^-				11.82	1				
1^-	5.79		6.58	6.10	1	0.1		0	0
1^-	8.72		10.09	10.08	1			0.1	0.1
2^-	4.97		5.12	4.54					
2^-			7.69	7.26					
3^-	5.62		5.83	5.44					
3^-	7.17		8.84	8.07					
4^-	7.01		7.55	6.79					
5^-	8.45		9.27	8.68					
5^-	(8.82)		12.78	11.79					
6^-	10.61		11.80	10.91					
7^-	13.33		13.56	12.99					
8^-	(15.62)		16.17	15.13					
9^-	15.18		16.47	15.89					

[a] Reference 9.
[b] Reference 18.

1^+, 3^+, and 5^+ states all have $p_{1/2}$-occupation values of 3.35. The second and third 1^+ and 3^+ states have values of ≈ 2, and could be called 4p-2h states. There is one 2^+ state in the *K-dsd* calculation, while there are two low-lying 2^+ states in the *pds* calculations, both with occupation probabilities near 2.5. This suggests that for these states the "spherical" and the 4p-2h "deformed" states are very mixed. (The experimental data, Table II, suggest there should be much less mixing.) The lowest 0^-, 2^-, 1^-, and 3^- levels have occupation values near 2.5, and are essentially 3p-1h states. A similar analysis of the $T=1$ states, in ^{18}O, suggest that the first and second 0^+ and 2^+ states and the first 3^+ and 4^+ states are "conventional" states, while the third 0^+ and 2^+ states are 4p-2h states.

The $p_{1/2}$-occupation values in ^{19}F are given in Table IX. They have been grouped into sets of states which can be referred to as rotational bands, and we see a clear distinction in these values in the different bands. In the ground-state band in *Z-pds*, the values are all in the region from 3.2 to 3.5. With the *F-pds* calculation, the values for the $\frac{1}{2}$, $\frac{5}{2}$, $\frac{9}{2}$, $\frac{11}{2}$, and $\frac{13}{2}$ states cluster around 3.0. As discussed above, the $\frac{3}{2}^+$ state is probably strongly admixed with the $d_{3/2}$ orbit which is omitted from this calculation. There is thus anomalously large core excitation in this state, $\langle Np_{1/2}\rangle = 2.34$, as a result of trying to fit the observed $\frac{3}{2}^+$ level. There is apparently considerable mixing between the two low-lying $\frac{7}{2}^+$ states in the *F-pds* model, leading to a somewhat low value for the $p_{1/2}$ occupation for the lowest $\frac{7}{2}^+$ level.

Above the ground-state rotational band, the levels can be conveniently grouped into three "bands", a $K=\frac{1}{2}^-$ band, a $K=\frac{3}{2}^+$ band, and a $K=\frac{3}{2}^-$ band. The $\frac{3}{2}^+$ bands have $p_{1/2}$ occupations consistent with a 5p-2h description, while the negative-parity bands are 4p-1h states, with slightly more 6p-3h admixture in the lower band.

It is not easy to characterize the low-lying states in ^{19}O in this fashion. The $p_{1/2}$ occupations do not suggest any obvious low-lying deformed

TABLE VII. Excitation energies and spectroscopic factors for the $A=20$, $T=1$ system.

	Energy (MeV)				$(2J+1)\times S$ factors for $^{19}\mathrm{F}\rightarrow A=20$, $T=1$ system		
					Expt.[b]	*K-dsd*	*F-pds*
J^π	Expt.[a]	*K-dsd*	*Z-pds*	*F-pds*	$l=2/l=0$	$l=2/l=0$	$l=2/l=0$
0	3.53	2.68	2.11	2.59	0/0.3	0/0.6	0/0.5
1	1.06	0.92	1.36	0.94	0/0	0/0	0/0
1	3.49	2.47	2.98	3.03	0/1.2	0/1.7	0/1.2
1		3.75	3.70	3.57	<0.1/0	0.2/0	/0
2	0	0	0	0	0/0	0/0	0.3/0
2	(2.04)	1.76	2.14	1.73	2.3/0	3.3/0	2.4/0
2	(3.59)	2.63	2.60	2.70	0.4/<0.4	0.1/0	0.5/0
2	(4.28)	3.86	4.10	3.62	0.1/0	0.2/0	0/0
3	0.66	0.61	0.27	0.45	2.6/0	4.7/0	3.9/0
3	(2.20)	2.26	2.25	1.76	0.5/0	0.1/0	0.4/0
3	(2.97)	2.43	3.79	3.51	0.4/0	0.1/0	0.2/0
3	(3.69)	3.55	4.06	3.86	0/0	0.4/0	0/0
4		1.21	0.68	0.78			
4		4.17	4.25	3.32			
5		2.29	1.74	1.64			
6		4.48	4.23	3.53			
0			2.92	2.87			
1	(0.98)		0.85	0.68			
1			3.52	3.45			
2	(1.31)		0.98	0.88			
2	(1.97)		1.43	1.43			
2			3.71	3.68			
3	(1.82)		1.41	1.51			
3	(3.17)		2.70	2.30			
3			4.14	4.02			
4	(2.87)		2.56	2.20			
4			4.12	3.70			
5			3.45	3.28			
6			5.50	4.93			

[a] Reference 9.
[b] Reference 19.

state in ^{19}O.

The $p_{1/2}$ occupations for ^{20}Ne are shown in Table X. There are several features of interest here. We list the three 0^+ bands. The first two bands all have $p_{1/2}$ occupations greater than 3.0 and can be classified as s-d-shell "bands," while the third band has an occupation value around 2.0. These results are reasonably consistent with information drawn from cluster-transfer experiments[15,16] which populate ^{20}Ne. The third band in ^{20}Ne is not populated in α transfer on ^{16}O, but it is populated in 2-α transfer on ^{12}C. This has led to describing the third band as an 8p-4h band. The occupation values around 2.0 for these levels in the calculated spectrum bring this description into question. The 4h state in ^{16}O, as calculated here, has a $p_{1/2}$ occupation of about 0.5. This all suggests that this third band has a large 6p-2h component. Roughly 30–40% of the wave functions for the states in this third band consist of configurations with four holes in the $p_{1/2}$ orbit, while states in the first two bands have less than 4% of the wave functions involving configurations with four $p_{1/2}$ holes. But this 30 to 40% 4h component may well arise from acting on the 30% 2p-2h component in the ^{16}O ground state with a 6p-2h operator to generate this third band.

Thus, the evidence from this type of analysis of the wave functions suggests the third band in ^{20}Ne in a 6p-2h band instead of an 8p-4h band. As pointed out above, the 8p-4h description arose because the states in this third band are populated in the (^{12}C, α) reaction on ^{12}C, but not in the α-transfer reaction on ^{16}O, and the tacit assumption was made that the cluster transfers are stronger when all particles are transferred into the same oscillator shell. There is no calculated evidence that this assumption is valid, and indeed there is evidence[20] that the opposite is true; i.e., that the spectroscopic factor for α transfer with two particles entering the p shell and two entering the s-d shell are comparable in size to the case where all four particles occupy the s-d shell.

TABLE VIII. $\langle N_{p_{1/2}} \rangle$ in ground states.

A	F-pds	Z-pds
^{16}O	3.26	3.20
^{18}F	3.21	3.36
^{18}O	2.62	2.75
^{19}F	3.14	3.31
^{19}O	2.90	3.10
^{20}Ne	2.93	3.24
^{20}F	3.36	a
^{20}O	2.65	3.0

[a]Not calculated.

There is one set of data which is somewhat difficult to reconcile with a 6p-2h description of this band; i.e., the data on the ^{22}Ne(p, t)^{20}Ne reaction[21] do not imply any strength to these "6p-2h" states, while the 6p-2h picture suggests the states should be seen. This is again somewhat hueristic, and only a detailed analysis of the 2p and 4p transfer reactions involving ^{20}Ne will shed real light on this question.

Table X shows that the $K = 2^-$ band states all have $p_{1/2}$ occupations close to 2.6, consistent with a 5p-1h description.

Returning briefly to the $p_{1/2}$ occupation in the ground-state band of ^{20}Ne, note that in both the Z-pds and F-pds calculations this value steadily increases with increasing J through the $J = 6^+$ state. This means that with increasing J, the rms radius of these states is decreasing, or there is "antistretching." This is in contrast to the concept in collective rotational models that the nucleus stretches as the "rotational frequency" increases, thus accounting for the bending over of the energies in rotational bands with increasing J.

As discussed above, the simplest Nilsson model picture of ^{20}F says there should be low-lying $K = 1^+$ 2^+, 1^-, and 2^- bands seen in the spectrum of this nucleus, and indeed the calculated levels in ^{20}F in the pds-model calculations appear with spins in sequences consistent with this picture. The $p_{1/2}$ occupations for the $K = 1^+$ and 2^+ bands are consistent with an s-d-shell nature for these states, and the $K = 1^-$ and 2^- bands are 5p-1h states. The lowest positive-parity states in the calculated spectrum outside these bands have

TABLE IX. $\langle N_{p_{1/2}} \rangle$ for states in ^{19}F.

$2\times J^\pi_i$	$\langle N_{p_{1/2}} \rangle$ F-pds	Z-pds	$2\times J^\pi_i$	$\langle N_{p_{1/2}} \rangle$ F-pds	Z-pds
1^+_1	3.14	3.31	1^-_1	2.40	2.53
3^+_1	2.34	3.18	3^-_1	2.41	2.55
5^+_1	3.04	3.26	5^-_1	2.40	2.54
7^+_1	2.64	3.25	7^-_1	2.39	2.57
9^+_1	3.24	3.44	9^-_1	2.40	2.53
11^+_1	3.24	3.44			
13^+_1	3.36	3.53	3^-_2	2.48	2.67
			5^-_2	2.37	2.59
3^+_2	2.26	1.88	7^-_2	2.42	2.63
5^+_2	1.60	1.86	7^-_2	2.51	2.75
7^+_2	2.14	2.03			
9^+_3	1.94	1.99			

$J=0^+$ and $J=2^+$ with $p_{1/2}$ occupations which imply that they are 6p-2h states.

The $p_{1/2}$ occupations for ^{20}O do not suggest any particulatly illuminating comments.

This discussion then implies that although the first excited band in the core states in ^{16}O is a 4p-4h state, in the nuclei with $A=18$, 19, and 20, all the low-lying deformed states are based on 2p excitations from ^{16}O. We have found no low-lying states in the mass 18, 19, and 20 systems for which the calculations imply a primarily 4h character.

V. COMPARISON WITH OTHER CALCULATIONS

There are a number of other calculations[22-27] which attempt to give a microscopic description of even- and odd-parity states in these light s-d-shell nuclei. We have already referred to Zuker's calculation for mass 18 which is essentially repeated here. Ellis and Engeland[24] have treated the mass region from $A=17$–19 in a weak-coupling model approach originally suggested by Arima, Horiuchi, and Sebe.[25] They obtain shell-model wave functions for up to 4p in the s-d shell and for up to 3h in the p shell. They thus include some effects due to the $d_{3/2}$ and $p_{3/2}$ orbits explicitly, while we include none. They then form states by weakly coupling the lowest appropriate h and p states to form states in the given nuclei. In the mass 18 and 19 negative-parity state calculations they consider in detail only 1h states, and in the positive-parity states in $A=18$, only 2h states. For the separate h and p calculations, they work in an SU(3) representation which is very convenient for truncation purposes. Our calculations for "1h" states and "2h" states give results similar to theirs. Our spectrum is richer above these states, obviously, since we include more multiparticle excitations. Benson and Flowers[26] have reported similar calculations with similar results.

Arima and Strottman[27] have calculated properties of ^{20}Ne in an SU(3) basis with up to 4h in the ^{16}O core, and they including excitation to the f-p shell. One of their conclusions is that the 7.2-MeV 0^+ state is most likely 4h in nature. We have pointed out that our calculated results describe this state as a 6p-2h state and we have also pointed out the difficulty in clearly resolving this discrepancy.

TABLE X. $\langle N_{p_{1/2}} \rangle$ for states in ^{20}Ne.

J^π_i	$\langle N_{p_{1/2}} \rangle$ F-pds	Z-pds	J^π_i	$\langle N_{p_{1/2}} \rangle$ F-pds	Z-pds
0_1	2.93	3.24	0_3	1.73	2.19
2_1	3.06	3.36	2_3	1.59	2.05
4_1	3.29	3.55	4_3	1.78	1.97
6_1	3.50	3.73	6_3	1.92	2.62
8_1	3.37	3.62			
0_2	2.50	3.06	2_1^-	2.34	2.55
2_2	2.53	3.44	3_1^-	2.35	2.57
4_2	1.73	3.50	4_1^-	2.37	2.62
6_2	2.11	2.83	5_1^-	2.42	2.66

VI. SUMMARY

We have presented here the results of a series of calculations of the structure of low-lying positive- and negative-parity states in the mass region $A=18$–20. The calculations were done in terms of a conventional spherical shell model, with ^{12}C treated as an inert core, and active particles in the $p_{1/2}$, $d_{5/2}$, and $s_{1/2}$ orbits. In these core-excited model calculations we used two different effective residual interactions. One was based on so-called realistic interactions derived from a nucleon-nucleon potential, and one was parametrized in terms of two-body matrix elements which were determined by observed excitation energies of states in nuclei from $A=13$–22. The single-particle energies used are consistent with the energies suggested by the spectra of ^{13}C and ^{13}N. It should be stressed that although these single-particle energies are quite different from the h-p energies around the ^{16}O core, the models do yield correct relative binding energies for the ground states of the $A=15$, 16, and 17 systems, so that the calculations are completely consistent with nature in this regard. The results of these calculations can be summarized as follows:

(1) With one model, the energies of almost all low-lying states of both negative and positive parity in the $A=18$ to $A=20$ nuclei are reproduced with almost quantitative accuracy. The calculations with the Zuker interaction can fairly be described as parameter free as far as this calculation is concerned. The F-pds calculation involved many parameters. The few differences between these two calculations imply that these results are not dependent on any fine details of the residual interaction. Within the accuracy one can expect for extracting spectroscopic factors by distorted-wave methods, the calculated spectroscopic factors are in equally good agreement with experiment.

(2) The calculated $p_{1/2}$ occupations suggest that

the degree of core excitation is not significantly affected by the addition of four particles going from ^{16}O to ^{20}Ne. The model does imply that there is a larger degree of core excitation in the oxygen isotopes than in the other nuclei treated. We know of no evidence that this is true in nature.

(3) None of the low-lying states in the calculations reported here can be called "4h" states, and we can offer no suggested experiment which would clearly distinguish between 2h and 4h states insofar as cluster-transfer experiments are concerned.

(4) The "rotational" features observed in these nuclei appear in a completely natural fashion. The fact that the wave functions for the ground-state "rotational band" in ^{20}Ne imply that the rms radius decreases with increasing J is in contradiction to the usual centrifugal stretching concept of the collective model.

(5) Insofar as the excitation energies and spectroscopic factors are concerned, the only direct consequence of our extreme truncation is a failure to describe the $\frac{3}{2}^+$ member of the ground-state rotational band in ^{19}F, which state obviously requires some $d_{3/2}$ single-particle admixture. There is no similar discrepancy which can obviously be ascribed to the omission of the $p_{3/2}$ orbit. The other main problem here is with the 2^+ states in ^{18}F, which still defy accurate description. One must always remember, too, that the center-of-mass spurious state problem has not been treated in any way here.

We are grateful to the following for numerous useful discussions during the course of this investigation: H. T. Fortune, A. Arima, and M. H. Harvey.

---

*Research sponsored in part by the U. S. Atomic Energy Commission under contract with Union Carbide Corporation.

†Research supported in part by the U. S. National Science Foundation.

[1]E. C. Halbert, J. B. McGrory, B. H. Wildenthal, and S. P. Pandya, in *Advances in Nuclear Physics*, edited by M. Baranger and E. Vogt (Plenum, New York, 1969), Vol. 4.

[2]A. P. Zuker, B. Buck, and J. B. McGrory, Phys. Rev. Letters 21, 39 (1968).

[3]A. P. Zuker, B. Buck, and J. B. McGrory, *Contributions to the International Conference on Properties of Nuclear States* (Univ. of Montreal Press, 1969), p. 193.

[4]A. P. Zuker, Phys. Rev. Letters 23, 983 (1969).

[5]J. B. McGrory, Phys. Letters 31B, 339 (1970).

[6]B. Reehal and B. H. Wildenthal, to be published.

[7]T. T. S. Kuo, Nucl. Phys. A103, 71 (1967).

[8]J. B. French, E. C. Halbert, J. B. McGrory, and S. S. M. Wong, in *Advances in Nuclear Physics* (see Ref. 1), Vol. 3.

[9]F. Ajzenberg-Selove, Nucl. Phys. A190, 1 (1972).

[10]L. M. Polsky, C. H. Holbrow, and R. Middleton, Phys. Rev. 186, 966 (1969).

[11]J. L. Wiza, R. Middleton, and P. V. Hewka, Phys. Rev. 141, 975 (1966).

[12]G. T. Kaschl, G. J. Wagner, G. Mairle, V. Schmidt-Rohr, and P. Turek, Nucl. Phys. A155, 417 (1970).

[13]L. L. Green, C. O. Lennon, and J. M. Naqib, Nucl. Phys. A142, 137 (1970).

[14]J. L. Wiza and R. Middleton, Phys. Rev. 143, 676 (1966).

[15]N. Marquardt, W. von Oertzen, and R. L. Walter, Phys. Letters 35B, 37 (1971).

[16]R. Middleton, in Proceedings of Heavy Ion Conference, Oak Ridge, Tennessee, 1972 (to be published); H. T. Fortune, *ibid.*

[17]P. Goode and S. S. M. Wong, Phys. Letters 32B, 89 (1970); S. Pittel, Phys. Letters 34B, 555 (1971).

[18]R. Siemssen, L. L. Lee, and D. Cline, Phys. Rev. 140, B1258 (1965).

[19]H. T. Fortune, G. C. Morrison, R. C. Bearse, J. L. Yntema, and B. H. Wildenthal, Phys. Rev. C 6, 21 (1972).

[20]A. Arima, private communication.

[21]W. R. Falk, R. Kulisic, and O. McDonald, Nucl. Phys. A167, 157 (1971).

[22]P. Federman and I. Talmi, Phys. Letters 19, 490 (1965).

[23]G. J. Borse and J. M. Eisenberg, Phys. Letters 22, 630 (1966).

[24]P. J. Ellis and T. Engeland, Nucl. Phys. A144, 161 (1970).

[25]A. Arima, H. Horiuchi, and T. Sebe, Phys. Letters 24B, 129 (1967).

[26]G. Benson and B. Flowers, Nucl. Phys. A126, 305 (1969).

[27]A. Arima and D. Strottman, Nucl. Phys. A162, 423 (1972).